

Investigation of Current Percolation Characteristics in Coated Conductors

L. B. Wang, G. You, K. R. Barraca, K. Waller, J. M. Mahoney, J. L. Young, and C. Kwon

Abstract— The IBAD and RABiTS coated conductors are investigated by variable temperature scanning laser microscopy (VTSLM). In 50 μm scanning step images, IBAD samples have more uniform current distribution than RABiTS samples, which is related to more uniform current flow and the smaller grain sizes in IBAD. The percolation cluster sizes are estimated to be 40 - 150 μm in IBAD and 50 - 150 μm in RABiTS. In the transition region, the current percolation is due to the combination of the grain boundary network and the critical temperature variation. At the temperature below the critical temperature, the images of VTSLM show that the current bottleneck area causes the major local dissipation limiting I_c . We also find that the dissipation areas have lower T_c^* and high δV_m , an important characteristic shared among all the lower J_c^* areas.

Index Terms—YBCO coated conductor, IBAD, RABiTS, Percolation.

I. INTRODUCTION

THE recent progress in the manufacture technology of the second-generation high temperature superconducting cable, YBCO coated conductors (CCs), has made the high electrical power application closer to the reality [1-4]. The critical current density (J_c) in CCs can approach that in single crystalline films. The higher J_c in CCs results from the better crystalline texture of YBCO. The texture of YBCO in CCs is initially created by ion-beam assisted deposition (IBAD) of an underlying buffer layer [5, 6], rolling assisted biaxially textured substrate (RABiTS) [7], and incline substrate deposition (ISD) [8] techniques. In the CCs, the crystalline texture reflects the variation of the grain boundary angles in YBCO film. As we know, the J_c is related to the grain boundary angles [9,10]. The higher the J_c is, the lower the grain boundary angles are. Due to the grain boundaries, the transport current is forced to flow across the sample by percolation [11,12].

In this paper, we use variable temperature scanning laser microscopy (VTSLM) to investigate the percolation

characteristics in IBAD and RABiTS CCs. We have estimated the size and the shape of percolation clusters from the both CCs. The percolation is formed from the combination of the variation in T_c and grain boundary angles. We have compared images in the superconducting states and the transition regions to find a relationship between the images.

II. EXPERIMENT

IBAD and RABiTS samples are prepared for four-probe transport measurements by depositing gold contacts. The platinum wires are soldered on the gold contacts by indium. The ac voltage data from the laser disturbance modulated by mechanical chopper are acquired by a lock-in technique. The temperature of the samples is controlled by a temperature controller in a cryostat. Detailed information about VTSLM can be found in our earlier publications [13,14].

III. RESULTS AND DISCUSSION

Fig.1 (a) is the temperature dependence of resistance in IBAD #1. T_c ($R = 0 \Omega$) is 90.6 K, and the transition width ΔT is about 1.3 K. Fig.1 (b) is the temperature dependence of resistance in RABiTS #1. T_c ($R = 0 \Omega$) is 90.3 K, and the transition width ΔT is about 1.3 K.

We have obtained VTSLM images Fig.2 (a) and Fig.2 (b) from IBAD #1 and RABiTS #1, respectively, when a 50 μm scanning step is employed at the middle of the resistive transition where we expect to get the largest signal (δV). In VTSLM images, δV is related to T_c and the local current density [14]. At the first glance, the signal δV represented with black and white is quite uniform in IBAD #1. This result indicates that the flow of the current is uniform and no significant variation of T_c exists in IBAD #1. Compared with IBAD #1, δV in RABiTS #1 is quite inhomogeneous. Such differences are consistently observed between IBAD and RABiTS samples.

We think that this difference is related to the grain sizes and the current percolation paths. Usually, the grain size of IBAD CCs is much smaller than that of RABiTS CCs which are as large as 100 μm [11]. Since the current flows percolatively via the paths determined by the grain boundary network in CCs, the feature size of the percolation path is related to that of the grain boundary network. Hence, IBAD is expected to have smaller feature size due to the percolation than RABiTS. Since Fig. 2 is taken with 50 μm scanning step, the step size is the limiting factor for the image resolution.

Manuscript received October 5, 2004. This work was supported by the Air Force Office of Science Research under Grant No.F49620-01-1-0493.

C. Kwon is with the Department of Physics and Astronomy, California State University, Long Beach, CA 90840 USA. (phone: 562-985-4855; fax: 562-985-7924; e-mail: ckwon@csulb.edu)

L. B. Wang, G. You, K. R. Barraca, K. Waller, J. M. Mahoney, and J. L. Young are with the Department of Physics and Astronomy, California State University, Long Beach, CA 90840 USA. (e-mail: wanglb1@yahoo.com; soileep@hotmail.com; kbarraca@yahoo.com; kauimaui@hotmail.com; jmattmahoney@hotmail.com; jeremyrainman@yahoo.com)

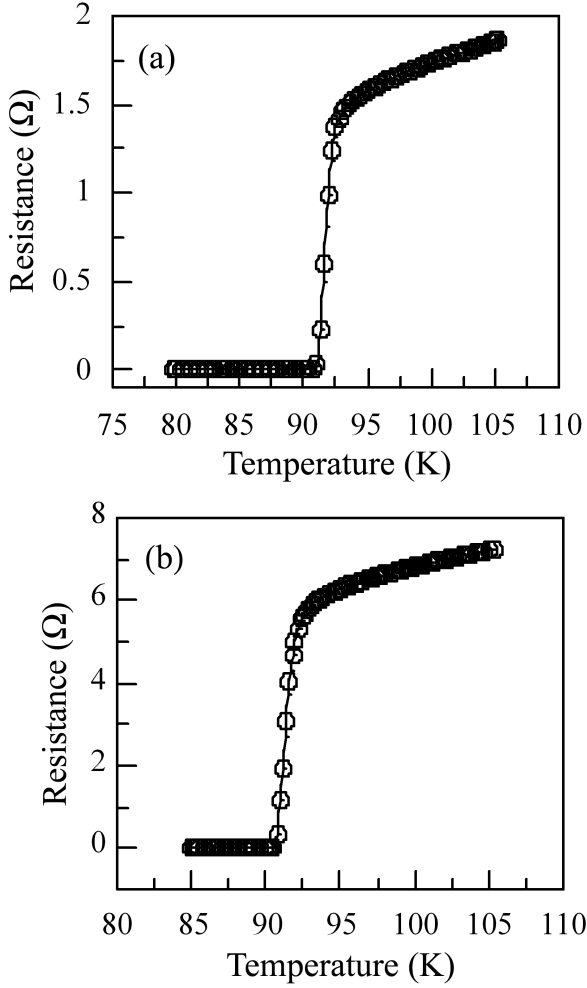


Fig. 1. The temperature dependence of resistance from (a) IBAD #1 and (b) RABiTS #1.

In order to investigate further, we have used smaller scanning steps to image IBAD and RABiTS CCs. As shown in Fig. 3 (a) and (c), the $3\ \mu\text{m}$ scanning step images reveal the features not observed in the $50\ \mu\text{m}$ images. While in RABiTS, the smaller scanning step images in Fig. 3(b) and (d) give higher resolution images but do not reveal any new features. We estimate that the percolation feature size of IBAD samples is about $40 - 150\ \mu\text{m}$, and that of RABiTS sample is about $50 - 150\ \mu\text{m}$; surprisingly they are in the same range. Since the feature sizes are similar, we have concluded that the main difference between IBAD and RABiTS is actually the variation of signals across the features. In IBAD, the signal does not change much across a feature while the change is quite large in RABiTS. We believe that the percolation features in RABiTS are related to the actual grain boundaries since the grain size of RABiTS is in the same order of magnitude; while the features in IBAD are formed from a collection of grain boundaries. Hence there is larger variation of δV in RABiTS across the VTSLM features than in IBAD where δV is averaged over many grains.

In Fig.3, we find that the features have mainly two different shapes. One is more round, while the other is elongated to one direction. Since the features in VTSLM images are due to current percolation, the shape is related to percolation paths, i.e. the grain boundary network. We find that the long axis of the elongated shapes is preferentially aligned along the current direction, which agrees with the expectation from the percolation as well as the expectation based on our computer simulation.

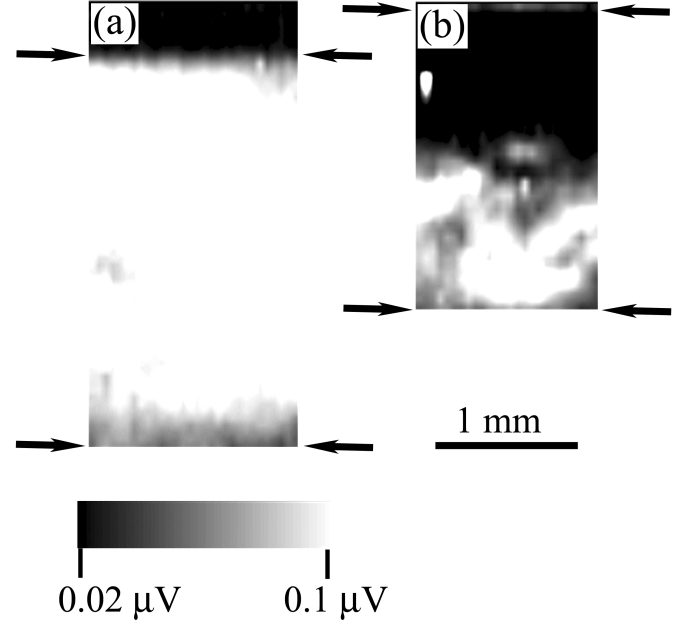


Fig. 2. VTSLM images at the middle of superconducting transition taken with $50\ \mu\text{m}$ scanning step. (a) IBAD #1 at 91.4 K, (b) RABiTS #1 at 91.2 K. The arrows represent the edges of the samples.

Fig. 4 shows the T_c^* and δV_m images of IBAD #1. In general, the variation of T_c^* is proportional to that of T_c ($R = 0\ \Omega$), the δV_m reflects the distribution of transport current [14]. Even though it is small ($< 0.4\ \text{K}$), some variation in T_c^* is observed. We have observed the variation in T_c^* from most of the YBCO films and CCs [13-15] confirming the difficulty of producing a homogeneous YBCO layer. The variation of T_c^* will be an additional factor to determine the percolation paths in CCs.

Even with grain boundaries, inhomogeneous T_c , and current percolations, many groups with different fabrication techniques have produced CCs with $J_c > 10^6\ \text{A}/\text{cm}^2$ signifying the importance of the macroscopic defects rather than the microscopic differences among CCs. Hence, we have begun to look for the macroscopic features limiting I_c in CCs and the diagnostic characteristics at higher temperature for the low J_c areas. Detailed data analysis is underway in order to understand how T_c^* and δV_m images are related to the current percolation and the current bottleneck in CCs. So far our study of various CCs has revealed that the area with large δV_m and lower T_c^* starts to have dissipation at lower current in the superconducting state, hence limiting the current carrying capability [15]. We think that the T_c^* in that area is reduced

because the locally increased current in the percolation path causes the resistive transition to shift to lower temperatures. It is interesting to point out that the areas with large δV_m but no reduced T_c^* do not appear to limit I_c . Hence, the large δV_m and lower T_c^* area can be interpreted as the bottleneck area where the current crowding occurs.

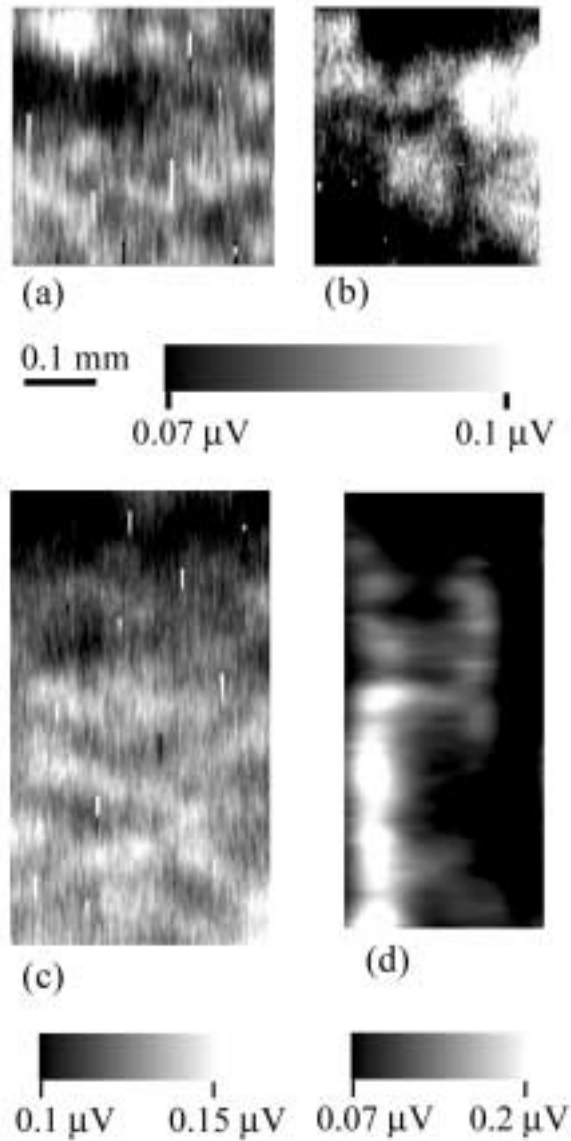


Fig. 3. VTSLM images of (a) IBAD #1 at 91.4 K by 3 μm scanning step, (b) RABiTS #1 at 91.1 K by 3 μm scanning step, (c) IBAD #2 at 91.2 K by 3 μm scanning step, (d) RABiTS #2 at 93.6 K by 10 μm scanning step. The current direction of (a), (b) and (c) is horizontal, while that of (d) is vertical.

As we discussed earlier, the VTSLM features in IBAD are generated by the percolation clusters and not by the individual grains. In order to investigate the relation between VTSLM features and the superconducting current transport in superconducting states, we have also studied IBAD in the superconducting temperature. Fig. 5 is the images of the IBAD #4 at different temperatures and bias currents. Two distinct areas are visible in the superconducting states shown in Fig.5 (a) and (b), a line-shaped area in the middle of the

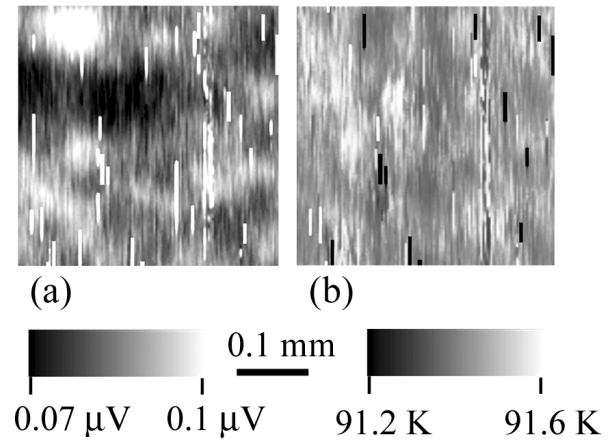


Fig. 4. (a) δV_m and (b) T_c^* images of IBAD #1 taken at the same as Fig. 3(a).

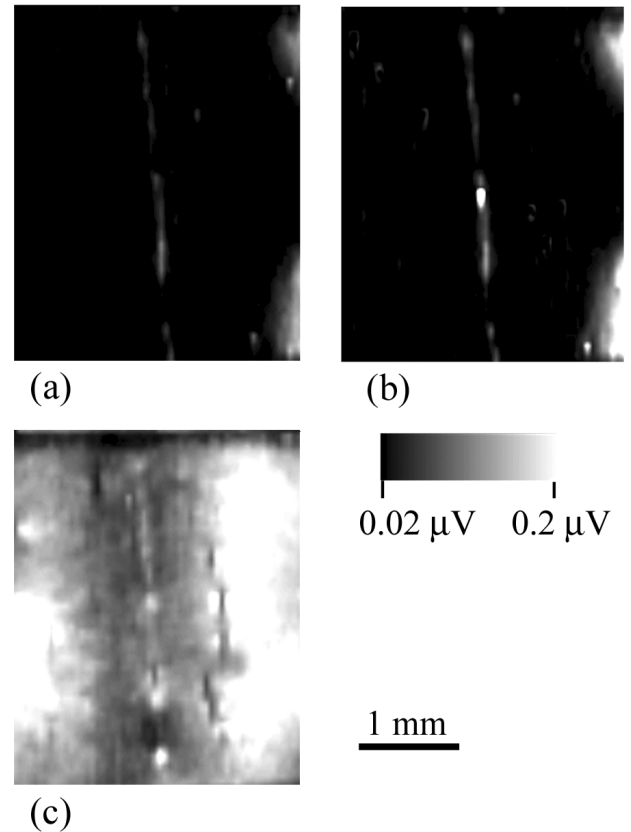


Fig. 5 VTSLM images of IBAD #4 taken when the sample is in the superconducting state at 90.0 K (a) with 90 mA and (b) with 100 mA and when the sample is in the transition (c) at 91.8 K with 5 mA.

sample and two strong δV areas in the right side of the sample. These images are taken at 90.0 K which is 0.6 K lower than T_c ($R = 0 \Omega$). In the superconducting state, δV usually indicates dissipation [16-18]. We calculate T_c^* and δV_m (not showing here) from 50 μm step images, and find that the strong signal areas of the right side have lower T_c^* and strong δV_m supporting our earlier statement. However, the line-shaped

dissipation in the middle is not distinctively noticeable in T_c^* and δV_m .

Fig. 5(c) shows an image obtained at a transition temperature. The signal in the right side of sample is strong, as expected from the comparison of J_c^* vs. T_c^* and δV_m . In addition, one can find the line-shaped feature where the dissipation occurred in Fig. 5 (a) and (b). We have checked the surface of the sample using optical microscopy, and found that there are some scratches in those positions. Further VTSLM measurements of the line-shaped dissipation area with a smaller step show (not shown) that there are a series of intermittent scratches across the sample and they are forcing the current to flow around them. In the high-resolution images, we find that the low J_c^* areas actually have low T_c^* and high δV_m even in the line-shaped dissipating area.

IV. CONCLUSIONS

In summary, some IBAD and RABiTS coated conductors are studied by VTSLM. The images taken in the transition region using 50 μm scanning steps show that the IBAD samples look more uniform than the RABiTS samples. This means that the current flows more uniformly in the IBAD samples than in the RABiTS samples. The feature size of the IBAD samples is estimated to be 40 – 150 μm , while that of the RABiTS samples is 50 – 150 μm . Since the features in VTSLM are caused by current density variation, we believe that the feature size is related to the percolation cluster sizes of the samples. We have established a relationship between the local dissipation in the superconducting state and the VTSLM images in the transition region; the low J_c^* areas have low T_c^* and high δV_m , which is due the current crowding and the existence of current bottleneck.

REFERENCES

- [1] S. R. Foltyn, P. N. Arendt, P. C. Dowden, R. F. DePaula, J. R. Groves, J. Y. Coulter, Q. X. Jia, M. P. Maley, and D. E. Peterson, "High-Tc coated conductors—performance of meter-long YBCO/IBAD flexible tapes," *IEEE Trans. Appl. Supercond.*, vol. 9, pp. 1519–1522, June 1999.
- [2] J. O. Willis, P. N. Arendt, S. R. Foltyn, Q. X. Jia, J. R. Groves, R. F. DePaula, P. C. Dowden, E. J. Peterson, T. G. Holesinger, J. Y. Coulter, M. Ma, M. P. Maley, D.E. Peterson, "Advances in YBCO-coated conductor technology," *Physica C*, vol. 335, pp. 73-77, June 2000.
- [3] V. Selvamanickam, H. G. Lee, Y. Li, X. Xiong, Y. Qiao, and J. Reeves, "Fabrication of 100 A class, 1 m long coated conductor tapes by metal organic chemical vapor deposition and pulsed laser deposition," *Physica C*, vol. 392, pp. 859-862, October 2003.
- [4] H. Iwai, T. Muroga, T. Watanabe, S. Miyata, Y. Yamada, Y. Shiohara, T. Kato, and T. Hirayama, "Investigation of high J_c $\text{YBa}_2\text{Cu}_3\text{O}_{7-x}$ coated conductors prepared by pulsed laser deposition on self-epitaxial CeO_2 buffers," *Supercon. Sci. Technol.*, vol. 17, pp. S496-S499, September 2004.
- [5] Y. Iijima, N. Tanabe, O. Kohno, and Y. Ikeno, "In-plane aligned $\text{YBa}_2\text{Cu}_3\text{O}_{7-x}$ thin films deposited on polycrystalline metallic substrates," *Appl. Phys. Lett.*, vol. 60, pp. 769-771 February 1992.
- [6] X. D. Wu, S. R. Foltyn, P. N. Arendt, W. R. Blumenthal, I. H. Campbell, J. D. Cotton, J. Y. Coulter, W. L. Hults, M. P. Mayler, H. F. Safar, and J. L. Smith, "Properties of $\text{YBa}_2\text{Cu}_3\text{O}_{7-\delta}$ thick films on flexible buffered metallic substrates" *Appl. Phys. Lett.*, vol. 67, pp. 2397-2399, October 1995.
- [7] A. Goyal, D. P. Norton, J. D. Budai, M. Paranthaman, E. D. Specht, D. M. Koreger, D. K. Christen, Q. He, B. Saffian, F. A. List, D. F. Lee, P. M. Martin, C. E. Kalbunde, E. Hatfield, and V. K. Sikka, "High critical current density superconducting tapes by epitaxial deposition of $\text{YBa}_2\text{Cu}_3\text{O}_x$ thick films on biaxially textured metal," *Appl. Phys. Lett.*, vol. 69, pp. 1795-1797, September 1996.
- [8] Y. Nakamura, T. Izumi, and Y. Shiohara, "Percolation analysis of the effect of tape length on the critical current density of 123 coated conductors," *Physica C*, vol. 371, pp.275-284, 2002.
- [9] D. T. Verebelyi, C. Cantoni, J. D. Budai, and D. K. Christen, H. J. Kim and J. R. Thompson, "Critical current density of $\text{YBa}_2\text{Cu}_3\text{O}_{7-\delta}$ low-angle grain boundaries in self-field," *Appl. Phys. Lett.*, 78, pp. 2031-2033, April 2001.
- [10] L. Fernández, B. Holzapfel, F. Schindler, B. de Boer, A. Attenberger, J. Hänisch, and L. Schultz, "Influence of the grain boundary network on the critical current of $\text{YBa}_2\text{Cu}_3\text{O}_7$ films grown on biaxially textured metallic substrates," *Phys. Rev. B*, vol. 67, pp. 052503-1-052503-4, February 2003.
- [11] Y. Nakamura, T. Izumi, and Y. Shiohara, "Percolation analysis of the effect of tape length on the critical current density of 123 coated conductors," *Physica C*, vol. 371, pp.275-284, 2002.
- [12] J. L. Reeves, D. M. Feldmann, C. Y. Yang, and D. C. Larbalestier, "Current barriers in Y-Ba-Cu-O coated conductors," *IEEE Trans. Appl. Supercond.*, Vol. 11, pp. 3863-3867, March 2001.
- [13] C. Kwon, L. B. Wang, S. Seo, B.H. Park and Q.X. Jia, "Spatial distribution analysis of critical temperature in epitaxial Y-Ba-Cu-O film using variable temperature scanning laser microscopy," *IEEE Trans. Appl. Supercon.* Vol. 13, pp. 2894-2896, June 2003.
- [14] L. B. Wang, M. B. Price, J. L. Young, C. Kwon, T. J. Haugan and P. N. Barnes, "Observation of nonuniform current transport in epitaxial $\text{YBa}_2\text{Cu}_3\text{O}_{7-x}$ film near the superconducting transition temperature," *Physica C*, vol. 405, pp. 240-244, June 2004.
- [15] L. B. Wang, P. Selby, C. Khanal, G. Levin, T. J. Haugan, P. N. Barnes, and C. Kwon, "The distribution of transport current in the YBCO coated conductor with zipper striations," *submitted to IEEE Trans. Appl. Supercon.*
- [16] R. Gross and D. Koelle, "Low temperature scanning electron microscopy of superconducting thin films and Josephson junctions," *Rep. Prog. Phys.*, vol. 57, pp. 651-741, 1994.
- [17] A. G. Sivakov, A. V. Lukashenko, D. Abraimov, P. Müller, A. V. Ustinov, and M. Leghissa, "Low-temperature scanning laser microscopy of individual filaments extracted from $(\text{Bi}, \text{Pb})_2\text{Sr}_2\text{Ca}_2\text{Cu}_3\text{O}_{10+x}$ tapes," *Appl. Phys. Lett.*, vol. 76, pp. 2597-2599, May 2000.
- [18] T. Kiss, M. Inoue, S. Egashira, T. Kuga, M. Ishimaru, M. Takeo, T. Matsushita, Y. Iijima, K. Kakimoto, T. Saitoh, S. Awaji, K. Watanabe, and Y. Shiohara, "Percolative transition and scaling of transport E-J characteristics in YBCO coated IBAD tape," *IEEE Trans. Appl. Supercon.*, vol. 13, pp. 2607-2610, June 2003.